

A NEW AUTOMATED TECHNIQUE FOR LEFT- AND RIGHT-VENTRICULAR SEGMENTATION IN MAGNETIC RESONANCE IMAGING

Amin Katouzian¹, Ashwin Prakash² and Elisa Konofagou^{1,3}

Departments of ¹Biomedical Engineering, ²Pediatric Cardiology and ³Radiology
Columbia University, New York, NY, USA
ak2432@columbia.edu

ABSTRACT

In this paper we present a new automated method for detecting endocardial and epicardial borders in the left (LV) and right ventricles (RV) of the human heart. Our approach relies on morphological operations on both binary and grayscale images. First, the standard power-law transformation is applied on the image. Then, a region of interest (ROI) is selected semi-automatically, followed by automated endocardial and epicardial border extraction based on the selected ROI. In order to get the endocardial contour, the transformed image is thresholded and the maximum area, which indicates the cavity, is selected. Finally, the edge detection is performed and the papillary muscles (PMs) are excluded via a convex-hull method. The epicardial boundary is delineated through a Threshold Decomposition Opening (TDO) approach along with morphological operations. The algorithm extracts the most precise myocardial and RV contours. Experimental results from three normal subjects are shown and quantitatively compared with manually traced contours by an expert. It is concluded that the method performs well in both endocardial and epicardial LV contouring as well as RV cavity detection.

1. INTRODUCTION

The endocardial and epicardial borders identification has been of extensive interest in medical image processing. The goal of the segmentation techniques is the automated detection of the LV boundaries in order to assist cardiologists in the detection and diagnosis of myocardial disease. Contrary to echocardiograms, the epicardial borders can be more clearly distinguished in Magnetic Resonance (MR) images and this has attracted recent research towards MR segmentation. Recently knowledge-based methods have been employed widely in segmentation applications as well as LV boundary detection [1-4]. In [5], the authors presented a new segmentation technique based on active appearance model (AAM), which is trained using a set of end-diastole (ED), mid-ventricular slices and minimizes the

error between the target and the synthesized image. In segmentation, all aforementioned algorithms have their own advantages, but, in their clinical applications, they have been only partially successful due to various reasons including:

- signal-to-noise ratio and image acquisition artifacts;
- misidentification of the border of fatty tissue as the epicardial border;
- irregularities in blood pool (cavity) boundary;
- dependence of myocardium and cavity shapes on type of disease, presence of PMs, slice and phase locations;
- inhomogeneity of the myocardium;
- image orientation;
- slice registration;

These factors along with constraints on existing algorithms, render the segmentation extremely challenging. For example, methods, which have to be either initialized using low-level contours or trained with a set of manually traced contours, might yield different results at different initializing or training parameters.

This paper is organized as follows. Section 2 describes the methods for LV and RV border detection. In section 3, the experimental results are shown and quantitatively compared to manually traced contours. Finally, the conclusion and a summary are given in section 4.

2. METHODOLOGIES AND ALGORITHM FOR BOUNDARY DETECTION

The methods behind our algorithm are morphological operations and image reconstruction in binary and grayscale images [6,7]. An initial reference point (marker), anywhere inside the blood cavity, has to be defined in the first image of the ciné-loop sequence. Then, a standard power-law transformation is performed and the ROI is selected using the marker. Morphological operations, thresholding and edge detection are used to delineate the RV and LV borders. In order to obtain the true oval-like shape of the short-axis

endocardial border, the convex-hull method is used in order to exclude the PMs.

2.1. ROI SELECTION

To begin with, an arbitrary reference point (marker) is defined somewhere inside the cavity, i.e., high intensity region of the LV. The power-law transformation ($I' = \kappa I^\gamma$) is then applied on the original image I , which is a mapping from an image of discrete plane Z^2 into a discrete set $D = \{0, 1, \dots, N-1\}$ of gray levels. Using this transformation, better differentiation between the muscle and the cavity is achieved and the myocardium contrast is enhanced. An additional benefit of this transformation is that the myocardium is completely isolated from fatty tissues, since the latter have relatively high intensity. The relationship between power-law transformation parameters shows that the span of the pixel values in the transformed image is sensitive to parameters κ and γ . Larger span hampers differentiation between cavity and muscle and smaller span makes epicardial border detection imperceptible. As a rule of thumb, κ and γ are selected as 1 and 1.3. The transformed image is then thresholded and small objects are removed while remaining objects are labeled. Given the position of the marker, the centroid of the cavity can be found and its label read. Subsequently, the centroids of all the objects and their pair-wise distances to the cavity's centroid are calculated. Since the RV is the nearest object to the LV cavity, the minimum distance, d_m discerns the centroid of the RV. A square window with its center at the centroid of the cavity and its length twice the minimum distance is used to automatically crop the ROI. Figure 1 shows the results of every step taken in the ROI selection procedure.

For the next image, the centroid of the cavity is considered

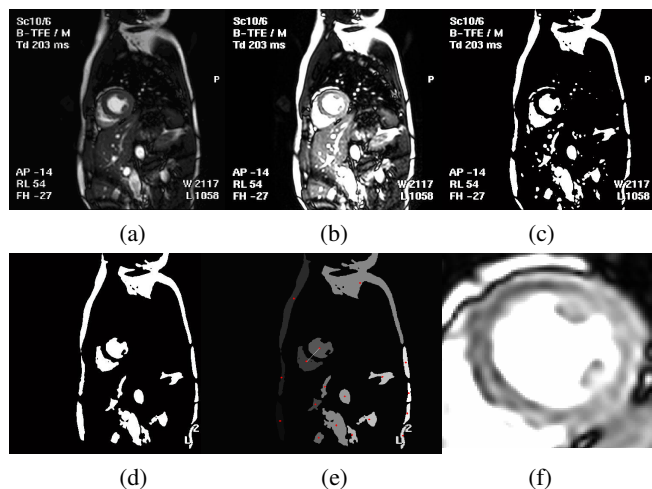


Figure 1. (a) an original short-axis view image. (b) power-law transformed image. (c) thresholded image. (d) thresholded image after small object removal. (e) labeled image with overlaid minimum distance (solid line). (f) selected ROI

as marker and the same procedure is repeated for all successive images. Using this method, the registration problem among slices is resolved because each time the marker is updated based on the previously identified LV cavity's centroid.

2.2. ENDOCARDIAL BORDER DETECTION IN THE LEFT AND RIGHT VENTRICLES

Conventionally, the endocardial wall motion, during a cardiac cycle, is one of the criteria used to diagnose myocardial disease such as infarction and ischemia. Hence, cardiologists use multiphase, multislice, cardiovascular MR images and extract the endocardial contours visually.

Automated detection of endocardial borders of LV and RV is not as challenging as epicardial because the LV and RV cavities have relatively high intensities compared to the myocardium and the surrounding tissues. Using thresholded image after small object removal, we can simply detect the endocardial borders in LV and RV using edge detectors given their labels (centroids). As we explained in section 2.1, the center point of the selected ROI is LV cavity's centroid and regardless of orientation of the short-axis view of the heart, the RV cavity's centroid would map to one of the four corners of the cropped ROI.

We take advantage of morphological operations in order to get rid of the irregularities in endocardial border of RV, especially in the septum area, which increase severely in phases close to end-systole (ES). Meanwhile, the presence and size of PMs is varied depending on the slice and the corresponding phase of the image. For instance, we can utilize convex-hull method to exclude those PMs, which appear in the border of the endocardium (mostly this happens in phases close to ES). This approach fails, however, when PMs are within the cavity. In order to deal with this issue, we use dilation and erosion operations using equal size structure element. Figure 2 shows the endocardial border of the LV and the smoothed RV border at the septum.

2.3. EPICARDIAL BORDER DETECTION

Three major problems are associated with epicardial border detection: inhomogeneous intensities, presence of fatty tissues and attachment of liver to the myocardium due to image acquisition artifact. Figure 1(f) shows the selected ROI of the power-law transformed image and the problems described are clearly visible.

In [7], Vincent extended the morphological reconstruction strategies in binary images to grayscale cases and demonstrated their applications and advantages for image filtering and segmentation. We apply this technique along with the Threshold Decomposition Opening (TDO) method to the power-law transformed image (Fig. 3(a)). In TDO,



Figure 2. selected ROI in thresholded image after small object removal (a). smoothed RV border at septum (b). endocardial border after edge detection (c). convex-hull of the endocardial border (d).

the binary opening operator \mathcal{O} , using a disk-structure element B , $B \subseteq I'_{ROI}$, is applied on the decomposed slices $T_k(I'_{ROI})$ of the selected power-law transformed image I'_{ROI} via recursive thresholding for $k=0, \dots, N-1$ such that:

$$T_k(I'_{ROI}) = \{p \in D, I'_{ROI}(p) \geq k\} \quad (1)$$

$$\forall p \in D, o(I'_{ROI}, B)_p = \max\{k \in [0, N-1] | p \in o(T_k(I'_{ROI}), B)\} \quad (2)$$

In each slice, the regional maximum is found and the opening operation is performed, which results in lowering the regional maximum if the area were not matched with the area specified by structure element. The size of the structure element is defined as half of d_m . By using TDO all intensities in the myocardium are preserved and the aforementioned problems resolved. Figure 3(b) shows the resulting image after performing TDO. The reconstructed image contains part of the RV. In this case, the smoothed RV is superimposed on the resulted image followed by thresholding (Fig. 3(c)) and edge detection (Fig. 3(d)).

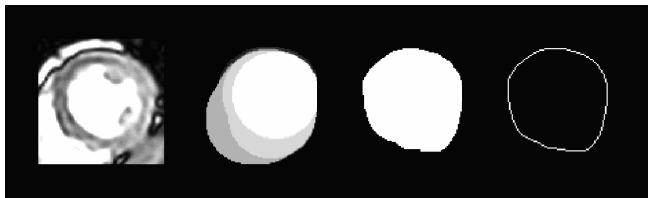


Figure 3. (a) selected ROI in power-law transformed image (b) same image in (a) after TDO; (c) thresholded image after complemented RV superimposing; (d) epicardial border delineation after edge detection.

3. QUANTIFICATION ANALYSIS

Our algorithm was tested on three normal subjects each set containing 300 (12 slices of 25 phases) short-axis view images of 256-by-256 pixels of size 1.44-1.79 mm. Figure 4 shows the automated segmentation results compared with the manually traced contours by an expert on three normal subjects at ES and ED phases.

In order to assess the performance of our method, linear

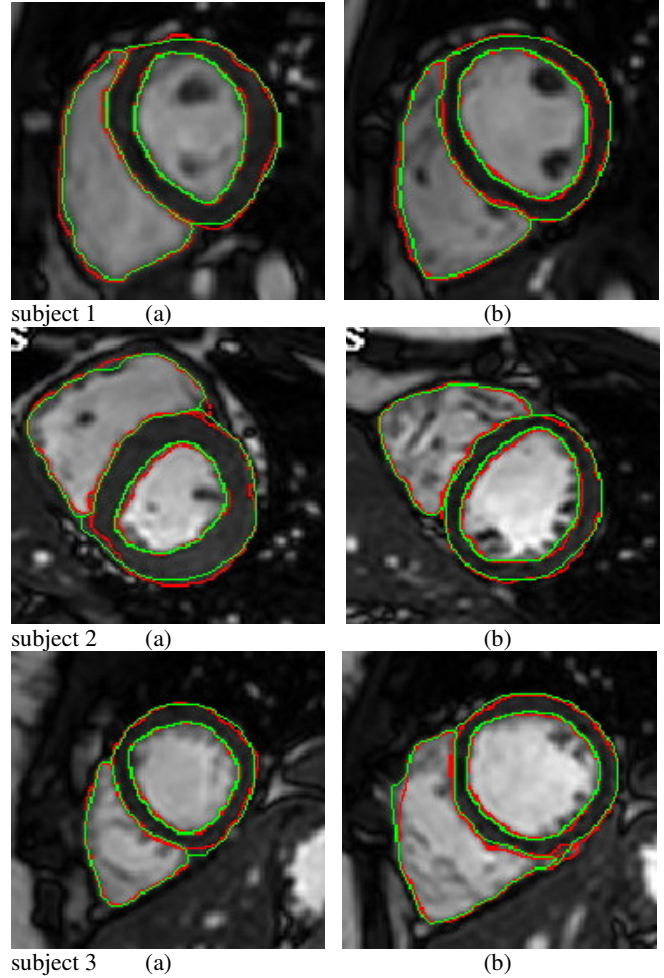


Figure 4. Comparison of automated (green) and manually (red) traced contours in three normal subjects. (images have been cropped manually in order to save the space). ES phase (a). ED phase (b).

regression analysis was performed and good correlation achieved among 70 images of automated and manually traced contours for LV borders of one normal subject (Fig. 5). In addition, in order to see how well our extracted contour is matched with the normal one regarding its position, the Tanimoto coefficient (η) was computed as follows:

$$\eta_{contour} = \frac{N_c^{contour}}{N_a^{contour} + N_m^{contour} - N_c^{contour}} \quad (3)$$

where, N_a, N_m are the number of enclosed pixels in automated and manually traced contours respectively and N_c is the number of common pixels in both. Figure 6 shows the Box-Whisker [8] plot of Tanimoto coefficients of endocardial and epicardial borders of LV with length of 1.5 times interquartile range.

4. RESULTS AND DISCUSSION

In this paper, we described a new algorithm using morphological operations and Threshold Decomposition

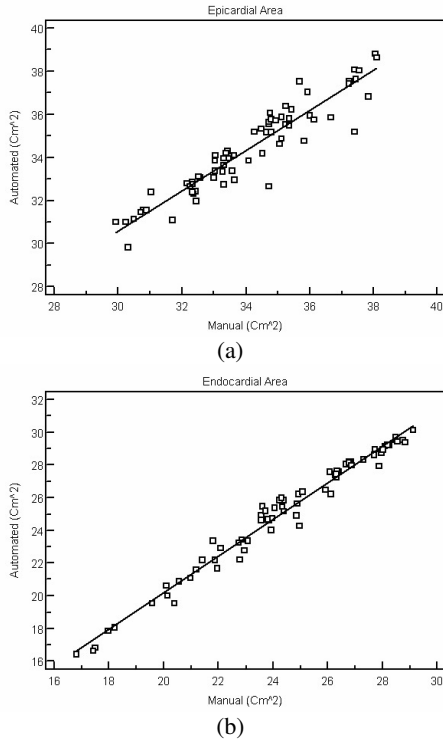


Figure 5. Comparison of the automated and manual traced contours in 70 images of one normal subject. LV Epicardial area:

$$r = 0.9396 \ (p < 0.0001), \ y = 0.9346x + 2.5393 \ (Cm^2) \ (a) \cdot$$

LV Endocardial area:

$$r = 0.9886 \ (p < 0.0001), \ y = 1.1238x - 2.2901 \ (Cm^2) \ (b) \cdot$$

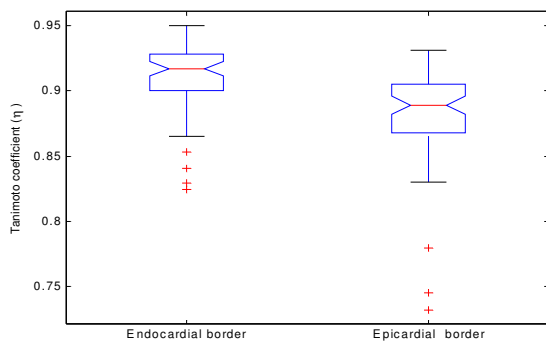


Figure 6. Box-Whisker plot of Tanimoto coefficient of LV borders.

Opening (TDO) method to identify LV and RV borders in the heart. We introduced a semi-automated method to select the ROI and enhanced the contrast of myocardium by applying the power-law transformation. We tested our algorithm on three normal subjects and compared the segmentation with manually traced contours in the case of one subject. Slices were chosen from half way between apex

and mid-ventricle to base. Regression analysis to evaluate the agreement between automated and manually traced contours showed the correlation of 0.9396 ($p < 0.0001$) and 0.9886 ($p < 0.0001$) between manual and automated segmentation for epicardial and endocardial borders of LV, respectively. In addition, we calculated the Tanimoto coefficients to see how well our automated and manually traced contours matched. The median Tanimoto coefficients were equal to 0.8891 and 0.9172 for epicardial and endocardial borders, respectively. These Tanimoto coefficients show the highest agreement in positioning of automated and manually traced contours for both diastolic and non-diastolic phases.

In this paper, we employed morphological operations and image reconstruction on both binary and grayscale images. We extended the application of morphological operation to cardiac image processing/segmentation and showed that how they might be used to detect the LV and RV borders of the human heart quickly and reliably. Currently, statistical evaluation on a complete set of individual subjects is being applied and the 3D models of the ventricles using extracted LV and RV contours will be reconstructed. In future, we will combine this technique as a preprocessing step with snake algorithm to reduce power-law transformation parameters sensitivity and improve stand-alone snake algorithm performance. Finally, the method will be tested on pathological cases along with the aforementioned quantification.

5. REFERENCES

- [1] T.F Cootes, C.J Taylor, D.C., J. Graham, "Active shape models - their training and application". *Computer Vision and Image Understanding*. Vol. 61, No. 1, pp. 38–59, 1995.
- [2] M. Leventon, W. Grimson, O. Faugeras, "Statistical shape influence in geodesic in active contours". *Proc. CVPR*. Pp. 316–323, 2000.
- [3] A. Tsai, A. Yezzi, W. Wells, C. Tempany, D. Tucker, A. Fan, W. Grimson, A. Willsky, "A shape-based approach to the segmentation of medical imagery using level sets", *IEEE Trans. on Medical Imaging* Vol. 22, No. 2, pp.137-154, 2003.
- [4] M. Rousson, D. Cremers, "Efficient kernel density estimation of shape and intensity priors for level set segmentation", *MICCAI*. pp. 757–764, 2005.
- [5] S.C. Mitchell, B.P.F. Lelieveldt, R.J. van der Geest, H.G. Bosch, J.H.C. Reiber, M. Sonka, "Multistage Hybrid Active Appearance Model Matching: Segmentation of Left and Right Ventricles in Cardiac MR Images," *IEEE Trans. Medical Imaging*, vol. 20, pp. 415–423, May 2001
- [6] L. Vincent, "Morphological Area opening and Closings for Greyscale Images," *Proc. NATO Shape in Picture Workshop*, Driebergen, The Netherlands, Springer-Verlag, September 1992.
- [7] L. Vincent, "Morphological Grayscale Reconstruction in Image Analysis: Application and efficient Algorithms," *IEEE Trans. Image Processing*, vol. 2, pp. 176-201, April 1993.
- [8] J. Chambers, W. Cleveland, B. Kleiner, P. Tukey, *Graphical methods for data analysis*, Belmont, CA: Wadsworth, 1983.